Adsorption of Alexa-Labeled Bt Toxin on Mica, Glass, and Hydrophobized Glass: Study by Normal Scanning Confocal Fluorescence

ARTICLE *in* BIOMACROMOLECULES · JUNE 2010

Impact Factor: 5.75 · DOI: 10.1021/bm100313n · Source: PubMed

Adsorption of Alexa-Labeled Bt Toxin on Mica, Glass, and Hydrophobized Glass: Study by Normal Scanning Confocal Fluorescence

Jean-Marc Janot,[†] Michel Boissière,[†,‡] Thierry Thami,[†] Emmanuel Tronel-Peyroz,[†] Nordine Helassa,[§,||] Sylvie Noinville,[⊥] Hervé Quiquampoix,[§] Siobhán Staunton,[§] and Philippe Déjardin*[,†]

Institut Européen des Membranes, Université Montpellier 2, UMR 5635 (ENSCM, CNRS, UM2), CC047, 34095 Montpellier Cedex 5, France, UMR 1222, Ecologie Fonctionnelle et Biogéochimie des Sols, INRA, Montpellier, France, and Laboratoire de Dynamique, Interactions et Réactivité, UMR 7075, CNRS, Thiais, France

Received March 22, 2010; Revised Manuscript Received April 26, 2010

We studied the kinetics of adsorption of alexa-labeled Bt toxin Cry1Aa, in monomer and oligomer states, on muscovite mica, acid-treated hydrophilic glass, and hydrophobized glass, in the configuration of laminar flow of solution in a slit. Normal confocal fluorescence through the liquid volume allows the visualization of the concentration in solution over the time of adsorption, in addition to the signal due to the adsorbed molecules at the interface. The solution signal is used as calibration for estimation of interfacial concentration. We found low adsorption of the monomer compared to oligomers on the three types of surface. The kinetic adsorption barrier for oligomers increases in the order hydrophobized glass, muscovite mica, acid-treated hydrophilic glass. This suggests enhanced immobilization in soil if toxin is under oligomer state.

Introduction

A large proportion of commercial crops of genetically modified plants synthesize the insecticidal protein known as Bt toxin originally produced by the soil bacterium *Bacillus thuringiensis*. The risks associated with the liberation of such toxins in the soil must be evaluated.[1] Bt toxin can be introduced into soil via decomposition of plant biomass and root exudation. The use of Bt crops can give markedly improved crop yields due to efficient protection against pests, but their use raises the question of exposure of nontarget organisms and resistance acquisition by target insects. The mineral composition of soil is greatly variable. The adsorption properties of various model minerals such as goethite, kaolinite, montmorillonite, rectorite, and silicon dioxide have been studied.[2−5] As for other proteins at interfaces, phenomena such as irreversible adsorption, conformational changes, exchange with other solutes, and pH dependence[6−9] are to be expected. Adsorption on soil may also increase the lifetime of the protein by physical protection against enzymatic degradation,[10,11] and it has been reported that insecticidal activity is conserved.[12] The aim of the present work is to contribute to the understanding of the fate of the toxin in the presence of hydrophilic minerals, such as muscovite mica and glass and hydrophobic surfaces via a surface-treated glass.

The state of the protein in solution is an important parameter in determining adsorption properties. When the protein concentration is high, high pH and high salt concentrations are required to inhibit polymerization.[13,14] Among the methods of preparation of the toxin reported in the literature, only a few verified that the monomer state was maintained in solution. The protein dimerizes easily[15] and so the monomer is difficult to maintain in solution. Although the tetramer is the entity responsible for the perforation of the insect midgut wall,[16] this tetramer is formed on the bilayer from monomers in solution. We present a study of the different adsorption behaviors of monomer and oligomers of a Bt toxin Cry1Aa. Sensitive detection on the surface was made possible by labeling the toxin with a fluorescent probe. We used slit geometry, as in a previous work with radiolabeled proteins,[17−19] to create controlled laminar flow. The solution signal is used for calibration to evaluate the interfacial concentration. In addition to the sensitivity obtained with a fluorescent label, the technique is useful in studies involving a mica surface, which is not suitable for other optical techniques such as total internal reflection fluorescence (TIRF), surface plasmon resonance (SPR), ellipsometry, or reflectometry.

Materials and Methods

Chemicals. The Cry1Aa solutions were prepared in 3-(cyclohexylamino)-1-propanesulfonic acid (CAPS, pK_a 10.4) and 3-(*N*-morpholino)-propanesulfonic acid (MOPS, pK_a 7.2). Both buffers were purchased from Sigma (France). Decyltrichlorosilane (Aldrich, France) and reagent grade toluene (Sigma, France) were used as received. Labeling of Bt was performed with Alexa-fluor-594 succinimidyl ester (InvitroGen, A30008).

Bt Toxin and Alexa-Labeled Bt. The procedure of preparation of Cry1Aa toxin has been published previously.[4] The protein (65000 g/mol) contains 609 residues and is composed of three distinct domains. The domain I contains eight helices bearing mainly negatively charged residues, while the stacked domains II and III are mainly composed of β-sheeted structures bearing positively charged residues so that the

* To whom correspondence should be addressed. E-mail: philippe.dejardin@iemm.univ-montp2.fr.
† UMR 5635.
‡ Present address: ERRMECe, UFR Sciences et Techniques, Université de Cergy-Pontoise, 2 avenue Adolphe Chauvin - BP222, 95302 Pontoise Cedex, France.
§ UMR 1222.
|| Present address: CNRS-IBS, LIM, 41 rue Jules Horowitz, 38027 Grenoble, France.
⊥ UMR 7075.

10.1021/bm100313n
Published on Web 05/07/2010

external protein surface has an uneven distribution of charges.[20,21] Its isoelectric point pI is 6.5.[22] Size determined by dynamic light scattering[4] was 7.2 nm. Aliquots of concentrated solution were provided in CAPS pH 10.5. Diluted samples in 10 mM CAPS, 350 mM NaCl, pH 9.6 were labeled with Alexa-594. Typically 800 μL of Bt solution were added to dry fluorophore Alexa-594 in molar ratio 1:1 and allowed to react for 1.5 h at 20 °C. The mixture was then put in an ad hoc microtube with filter (Biospin P6) and centrifuged at 16000 g for 1 min according to the supplier of the kit (InvitroGen). Elution of the filtrate on a preparative size exclusion chromatography column (BioRad P60; same elution buffer; pH 9.6) provided the pure monomer with no unreacted free label. It was verified that labeled and unlabeled samples presented the same elution curve. The final average labeling ratio [Alexa]/[protein monomer] was 0.5−0.7. When the mixture was submitted to chromatography without previous centrifugation, a substantial amount of oligomer was obtained with labeling ratio ≈ 0.1. Labeling ratio was determined from the UV absorbances at 277 nm where both the label ($\varepsilon_{277\text{-Alexa}} = 47793\ M^{-1}\cdot cm^{-1}$) and protein ($\varepsilon_{277\text{-protein}} = 82000\ M^{-1}\cdot cm^{-1}$) absorb and at 587 nm where only the label ($\varepsilon_{587} = 78000\ M^{-1}\cdot cm^{-1}$) absorbs. The difference between the labeling ratios can be explained by many nonaccessible labeling sites for the oligomers with probably specific parts exposed to surroundings.

According to column calibration with standard proteins, the apparent molar mass was 44000 g/mol for the monomer, lower than the reported value of 65000 g/mol. This may be attributed to an interaction with the column. A similar underestimation of the molar mass has been reported with another type of column in size exclusion chromatography HPLC analysis.[13] Oligomers were estimated to be an assembly of at least 10 monomers. Tubes were stored at +4 °C. The samples were diluted (0.1−1% in vol) immediately before adsorption in 50 mM NaCl, 10 mM CAPS buffer at the required pH, obtained by addition of HCl or in 50 mM NaCl, and 10 mM MOPS buffer for experiments at both pH 6.3 and 7.2.

Substrates. *Hydrophilic Surfaces.* Muscovite mica was purchased from Metafix SA (Montdidier, France) as 5 × 2 cm sheets. It was freshly cleaved before each experiment. Glass surfaces were microscope slides (Menzel-Glaser 25 × 60 mm) of thickness 140−150 μm. They were made very hydrophilic with acid treatment (H_2SO_4/30% w H_2O_2 70/30 vol at 90 °C for 30 min) followed by extensive washing with ultrapure water. The sessile water drop (surface tension 71.6 mJ/m^2 measured by the Wilhelmy plate technique) contact angle was near 0° with[23−25] ≈5 × 10^{14} silanols per cm^2. The acid-treated cleaned glass will be called "hydrophilic" in what follows to emphasize the contrast with hydrophobized glass.

Hydrophobized Glass. Glass slides after the previous treatment were dried under nitrogen flow and heated at 110 °C in an oven for 20 min. Then six slides, using a holder made in Teflon, were put in decyltrichlorosilane 1 mM in toluene (250 mL) at 20 °C for 1.5 h before rinsing with toluene (three times) and drying under nitrogen. The contact angle of distilled water sessile drop was 103.0 ± 0.9° over the six slides. Eight measurements, over the entire surface, were performed on each plate with narrow distribution (±0.5°), showing very homogeneous treatment on the whole surface of each item.

Flow Cell. The flow cell has been described previously.[26] A microscope slide, just cleaned or hydrophobized, was positioned near the objective. The other wall was mica sheet with holes punched at each extremity for entry and exit of flowing solution (Figure 1). The channel width w and height b were 3 mm and 50−70 μm, respectively. The parameter characterizing the convection is the wall shear rate γ deduced from the imposed flow rate Q according to the Poiseuille-like relation $Q = (1/6)\gamma b^2 w$. Experiments were carried out at $T = 19$ °C and $\gamma = 1000\ s^{-1}$ for 30 min or more. Flow occurs in the x direction normal to the y scanning direction. A typical experiment consisted of two stages: in the first, buffer flowed through the cell to obtain the background signal, and then the protein solution was introduced.

For technical reasons, the experimental setup was limited to about 60 μm between the slit walls. The flow was laminar as the Reynolds

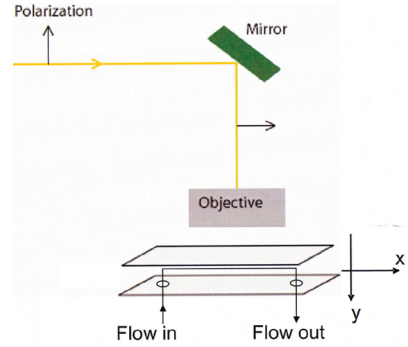

Figure 1. Schematic illustration of the directions x of flow and y of translation of the objective leading to the focus scanning through the thickness of the slit between the two walls of glass (top) and mica (bottom).

number was very small. During initial adsorption (weak concentration in the solution near the surface for high adsorption constant), coupling between convection and diffusion creates a depletion layer, the thickness δ_{depl} of which can be estimated from the transport-limited Lévêque model[27−29] of kinetic constant $k_{Lev} = 0.54\ (D^2\gamma/x)^{1/3}$: $\delta_{depl} \approx 1.86\ (Dx/\gamma)^{1/3} = 19\ \mu$m, with Bt diffusion coefficient $D = 5.6 \times 10^{-7}$ cm^2 s^{-1}, deduced from the Stokes−Einstein relation ($D = k_BT/(6\pi\eta r)$; k_B is the Boltzmann constant; η is the liquid viscosity; r is the radius of the protein; $x = 2$ cm; $\gamma = 1000\ s^{-1}$. For not completely transport-limited adsorption, such thickness remains of the same order of magnitude.[29−31] A rigorous simple analysis of the initial adsorption rate would require a ratio of 2−3 for half the thickness of the channel over the Lévêque depletion layer thickness. The present conditions with the ratio 1.5 could introduce interference between the two interfaces. However, we found this interference to be small, as the adsorption kinetics on mica were very similar in front of a strongly and mildly adsorbing wall. The transition from buffer to protein solution did not show a sharp profile, presumably owing to axial diffusion in the supply tubing and to the type of slit entrance. As the conditions were very similar between experiments, these drawbacks should not prevent the comparison between monomer and oligomers and between the different surfaces. Work is in progress to improve the transition from buffer to protein solution supply, to approach the almost step function obtained in a radioactivity cell[32] used for adsorption studies of α-chymotrypsin on mica.[18]

Optical Device. The optical device was previously described,[26] however, easier scanning was obtained as the step-by-step motor was changed to a piezoelectric device. A better separation of excitation and emission wavelengths was also obtained (SemRock NF01-594-25). The normal orientation of scanning with respect to the flow direction is sketched in Figure 1. The laser power was 500 nW, corresponding to a power density, when focused at the interface, of less than 180 W/cm^2, owing to the energy loss through the objective. Despite this relatively low energy, the x position of the sample was shifted a few micrometers (typically 5 μm) between each scan to avoid any possible contribution of photobleaching, an effect sometimes observed at higher laser power without lateral shift. Typically 200 scans along the y direction were performed at positions x between 2 and 2.1 cm from the hole of entrance. The correction for the variation of position along the x axis was negligible as the transport-controlled adsorption rate for an ideal slit varies with the (1/3) power of distance x to entrance.

Determination of Interfacial Concentration. Scanning normal to the walls of the slit through the solution provided a data set $F(y,t)$, corresponding to the counting of photons over some time δt at successive positions y, with a dependence $\delta t(y)$. The positions y were not regularly spaced, as large signal variations near the interface required a greater density of points than in the center of the slit. One scan over the slit thickness lasted 30−40 s. All the results presented were obtained by linear interpolations between the scan data to obtain instantaneous fluorescence signal profiles at defined time intervals. Figure 2 illustrates

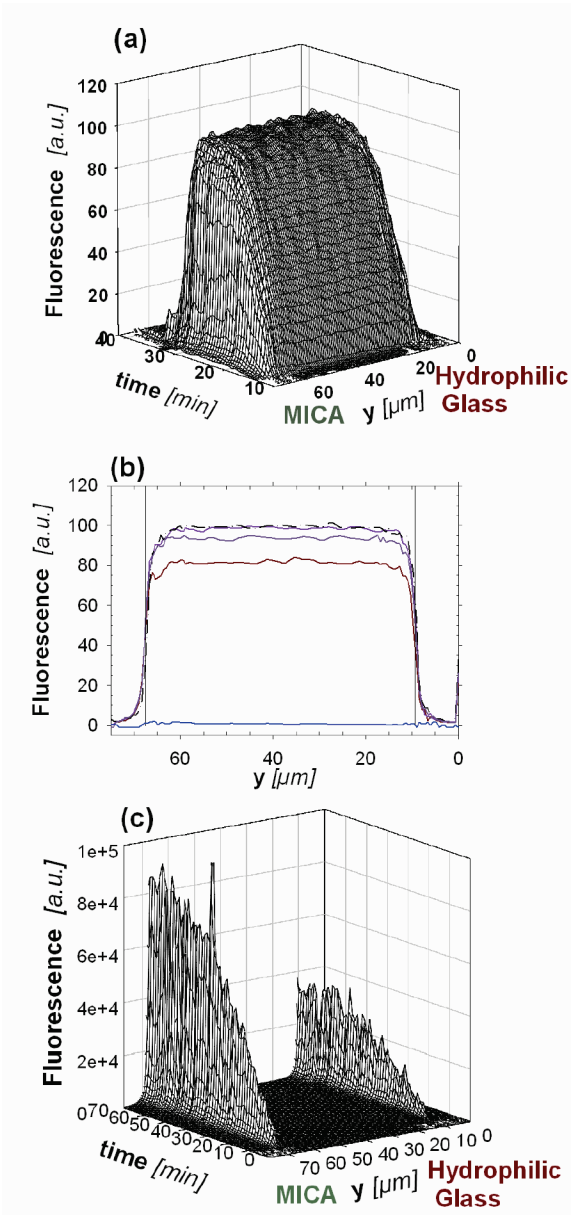

Figure 2. (a) Fluorescence concentration profile between walls of hydrophilic glass ($y = 9$ μm) and mica ($y = 67$ μm) as a function of time when no adsorption occurred (flowing of Alexa-labeled Bt solution at 2.0 μg/mL in 10 mM CAPS pH 10.5, 350 mM NaCl). (b) Shape of solution signal at the interfaces when no adsorption occurred; from bottom to top $t = 12.9$ (arrival of solution), 20, 22.7, 25, and 28.3 min. (c) Example when adsorption occurred (flowing of oligomers solution 6.6 μg/mL, pH 7.2).

typical interpolated profiles $F(y,t)$ without (Figure 2a) and with (Figure 2c) adsorption at the interfaces. The interfacial concentration was estimated by calibration given by the fluorescence signal F_{sol} of solution of known concentration C_b. F_{sol} was the final steady-state value of the solution signal in the cell when the concentration in the liquid phase was equal to the concentration of the incoming solution. The solution signal was always taken at mid-distance between the walls, because near the interfaces, the adsorption intense signal masked the true contribution of solution. F_{sol} was relative to an effective volume V containing solution at concentration C_b, while the signal F_{surf} from the surface concerned interfacial concentration Γ over area A. As a first approximation, we assumed that the fluorophore was randomly oriented at the interface as in solution. Then we had time (t)-dependent interfacial signal $F_{surf}(t) \propto \Gamma(t)A$ and calibration solution signal $F_{sol} \propto C_b V$ with the same proportionality constant. Therefore, $\Gamma(t) = (V/A)(F_{surf}(t)/F_{sol})C_b$.

Based on focus radius r_{focus} of 300 nm $\approx \lambda/2$ (objective numerical aperture $\omega = 1.2$; $\lambda = 594$ nm; $r_{focus} = 0.61\ \lambda/\omega$) and volume $V \approx 1$ μm^3, area $A \approx \pi r_{focus}^2$ and $V/A \approx 3.5$ μm. This gave only an order of magnitude, but V/A was constant for all experiments. Therefore, it allowed comparison between monomer and oligomers and between the different surfaces, which was the main purpose of the work.

The convolution of the solution profile (step function at both interfaces) with the beam shape led to a sigmoid at the interfaces with half the bulk solution signal at the interface (Figure 2b). We used then as surface signal F_{surf} the raw signal minus half the solution signal. This correction was negligible when a strong adsorption occurred at small solution concentrations.

The use of confocal fluorescence to monitor adsorption kinetics may introduce difficulties compared to studies using γ-radiolabeled protein where the calibration is provided by the solution signal jump.[33] The γ-emission and detection do not depend on the position of the protein, in solution or at the interface, nor is it dependent on its conformation and orientation. Conversely, the fluorescence properties may present such dependences. The orientation of the protein in solution is isotrope, but the surface may induce a preferred orientation of the adsorbed protein. Orientation changes can appear depending on surface coverage during the adsorption process.[18,31,34−37] Such considerations are relevant for a fluorophore firmly attached to the molecule.[26] In the present study, the labeling was performed to allow fluorophore freedom of rotation with respect to protein in solution. We assumed that such freedom or random orientation existed at the interface and that the surface had no effect on the spectroscopic properties of the molecule.

Results and Discussion

Influence of pH on Bt Adsorption (2.0 μg/mL) in CAPS. No adsorption occurred onto either interface (Figure 2a) when 2 μg/mL Bt solution in 350 mM NaCl, 10 mM CAPS buffer (pH 10.5) was flowing through the slit between mica and hydrophilic glass. Lower salt concentration (50 mM) at pH 8 and 7.3 (by addition of concentrated HCl) led to the same observation. Only at pH 6.3 a small amount was adsorbed at both interfaces. Conversely, on hydrophobized glass, we observed a small fluorescence signal at pH 10.5 and a much larger one at pH 6.3. From these series of experiments, it was inferred that significant adsorption occurred only close to the isoelectric point of the protein. We present below results of experiments at pH 6.3 and 7.2 for the adsorption of the protein as monomer and oligomer. To maintain significant buffering power of solvent in this range of pH, MOPS was used instead of CAPS as buffer, preferably to phosphate, as the dianions may introduce specific effects like promoting adsorption.[9]

Monomer Adsorption Kinetics. We studied adsorption from solutions at pH 6.3 using as buffer 50 mM NaCl and 10 mM MOPS (Figure 3). In such conditions, the Debye screening length (1.3 nm) is smaller than the protein size (7.2 nm). Therefore, the electrostatic interactions between protein and surface should be of relatively short-range and involve only a part of the molecule. On mica, a plateau concentration was observed at 20 μg/mL after 30 min, whereas a steady-state value was not attained at lower concentrations within 50 min. The adsorption kinetics may be expressed by an equation of the type $\Gamma = \Gamma_{max}[1 - \exp(-t/\tau)]$, at least over the time range of this study. In contrast, the adsorption behavior of Bt on hydrophilic glass showed an initial rapid step followed by a much slower one: the two hydrophilic surfaces can be considered as two different classes of surfaces for the toxin Bt.

After 1 h, the amount adsorbed was almost the same on mica and hydrophilic glass, 0.015−0.020 μg cm^{-2} for 5.3−20 μg/mL solution. The same level was attained on hydrophobized glass with the lower concentration of 2.0 μg/mL (Figure 4).

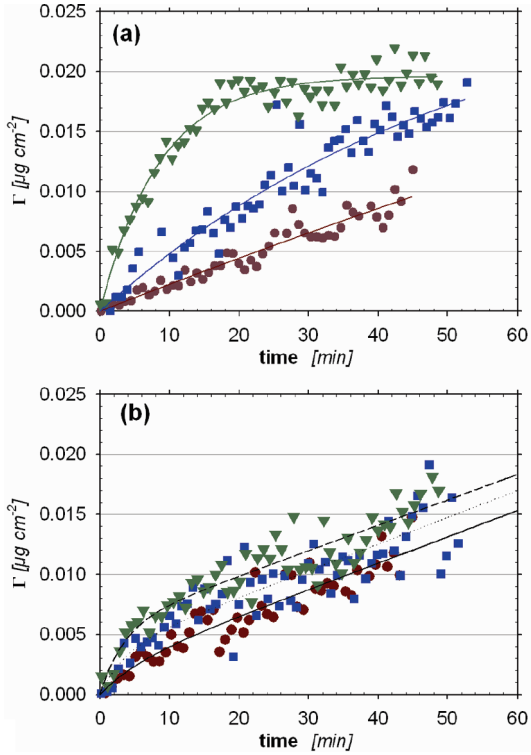

Figure 3. (a) Adsorption kinetics at pH 6.3 of monomer Bt on mica. From bottom to top: C_b = 3.3 (red circles); 5.3 (blue squares); 20 μg/mL (green triangles); (b) same as (a), except on hydrophilic glass.

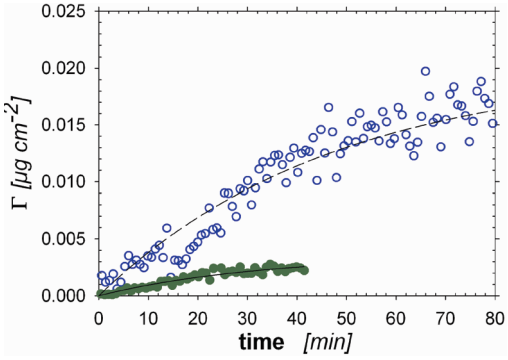

Figure 4. Adsorption kinetics from 2.0 μg/mL solution of monomer Bt on hydrophobized glass at pH 6.3 (open symbols) and pH 7.2 (full symbols).

Based on a first-order kinetic equation, the initial kinetic constant $(3.5 \pm 0.5) \times 10^{-6}$ cm s^{-1} (Figure 4; pH 6.3; open symbols) was higher than on mica $(2.3 \pm 0.1) \times 10^{-6}$ cm s^{-1} and hydrophilic glass $(2.0 \pm 0.5) \times 10^{-6}$ cm s^{-1} (from initial slope vs concentration according to Figure 3a and b, respectively). Those results suggested a slightly lower adsorption barrier of Bt monomer in the presence of hydrophobized surfaces compared to hydrophilic ones. In addition, on the hydrophobic substrate, the interfacial concentration decreased sharply as a function of pH above the isoelectric point of the protein (Figure 4).

Oligomer Adsorption Kinetics. Two series of experiments were carried out, one at pH 6.3, with Bt concentration of 13.2 μg/mL, and the other at pH 7.2, with half that concentration, namely, 6.6 μg/mL. Each series comprised two experiments, with mica facing either hydrophilic glass or hydrophobized glass. Adsorption kinetics are presented in Figure 5. There was no noticeable effect of the opposite wall on adsorption on mica,

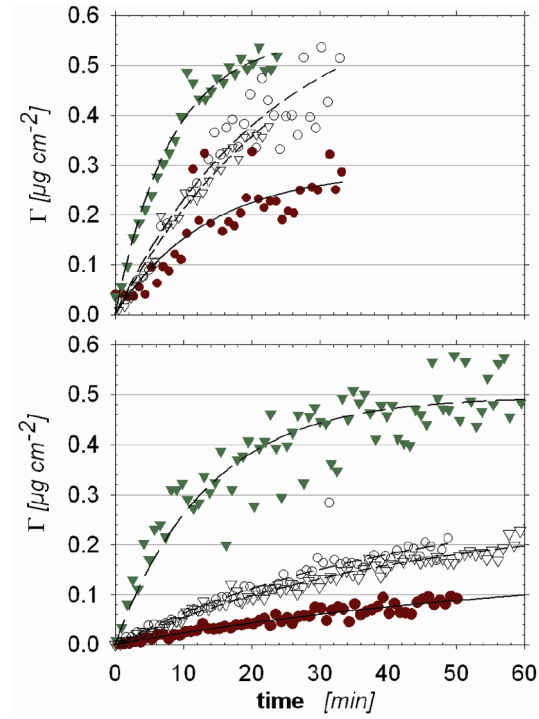

Figure 5. Adsorption kinetics of the oligomers on mica (○) in front of hydrophilic glass (red circles) and mica (▽) in front of hydrophobized glass (green triangles) from 13.2 μg/mL solutions at pH 6.3 (upper graph) and from 6.6 μg/mL solutions at pH 7.2 (lower graph).

as seen by the very similar kinetic curves. This was a confirmation of the absence of interference between the two interfaces in the adsorption process.

Whatever the pH value, adsorption onto mica was always intermediate between that on the two types of glasses. At pH 6.3, however, the differences between the surfaces tended to vanish, especially between mica and hydrophobized glass. Moreover, the final concentrations at both pH values for hydrophobic glass suggested the same limit of interfacial concentration probably close to surface saturation. Given the size of the monomer (assumed to be a sphere of diameter 7.2 nm), a hexagonal compact coverage of the surface would correspond to 0.24 μg/cm^2 and according to the random sequential adsorption model[38,39] to 0.14 μg/cm^2. In addition, there was the question of the extent of spreading of the oligomers on the surface. Whatever the exact value, it remained close to the order of magnitude of a monolayer of monomer or oligomers. To distinguish the pH effect from experiments carried out at concentrations differing by a factor two, the data shown in Figure 5 (fit curves, for sake of clarity) were presented in Figure 6 with the time scale axes for the two series differing by the same factor.

The pH had a small effect on the initial adsorption kinetics on hydrophobic glass, while the adsorption rate decreased markedly with increasing pH on mica and hydrophilic glass. The electrostatic interactions between the protein and the hydrophobic surface were not predominant in this range of pH. With a net negative charge on the protein above the isoelectric point, the more negative surfaces of mica and glass contributed a repulsive component for adsorption. Another way to illustrate the pH effect is to compare the initial value of the kinetic constants $(1/C_b)(d\Gamma/dt)_{t=0}$ (Figure 7): the constant in the presence of hydrophobized glass does not vary much between pH 6.3 and pH 7.2, while it decreased with increasing pH for both mica and hydrophilic glass. All these values were underestimated

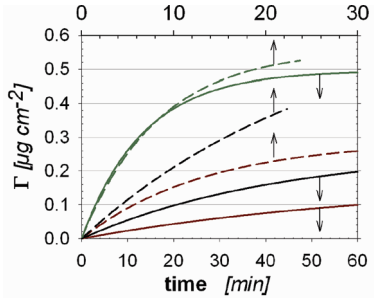

Figure 6. (Bottom time scale) Interfacial concentration of oligomers as a function of time at pH 7.2, $C_b = 6.6$ μg/mL (full lines from bottom to top: hydrophilic glass, mica, hydrophobized glass); (Top time scale) pH 6.3, $C_b = 13.2$ μg/mL (dashed lines: same order).

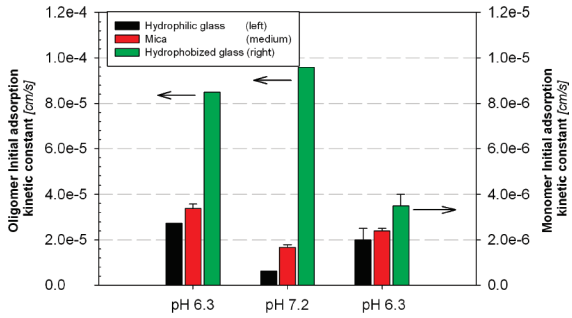

Figure 7. Initial kinetic constants for oligomers (left scale) and monomer (right scale) adsorption on hydrophilic glass, mica, and hydrophobized glass at pH 6.3 and 7.2.

because of the smooth transition from buffer to solution, but true values would follow the same order because hydrodynamic conditions were similar for all experiments.

Comparison between Monomer and Oligomers Adsorption. From the previous results it is clear that the adsorption properties of labeled monomer and oligomers were very different: (i) much faster adsorption occurred for the oligomers than for the monomer over the three types of surfaces and (ii) in the period of 30−50 min, oligomer adsorption was about 10 times greater than that of the monomer.

Although most measurements were not continued until a plateau value was attained, it is very likely that the plateau values for monomer would not attain the order of magnitude of the values for oligomers, unless surface-induced conformational changes occur over larger time scales. The surface was thus very far from full coverage. In the absence of deformation, the model of packing of hard spheres of radius r leads to interfacial concentrations varying as mass ($\propto r^3$) over area ($\propto r^2$). Thus, for a spherical oligomer of n monomers ($n \propto r^3$), the interfacial concentration varies smoothly with n as $n^{1/3}$. We observed indeed that the magnitude of the plateau observed for oligomers (0.5 μg cm^{-2}) was of the same order as the theoretical full coverage plateau for close packing of monomers (0.24 μg/cm^2).

The initial adsorption kinetic constant of oligomers was much larger than that of monomer. Based on transport-controlled processes where adsorption rate varies as $D^{2/3}$, a slower adsorption process would be expected for oligomers, contrary to experiments. Estimation of the transport-controlled process for a monomer of diffusion coefficient $D = 5.6 \times 10^{-7}$ cm^2 s^{-1} is k_{Lev} (monomer) $= 2.9 \times 10^{-4}$ cm s^{-1}, which was 100 times the observed value. Therefore, it was likely that the monomer adsorption was not controlled by transport. Conversely, the initial adsorption kinetic constant of oligomers on hydrophobized glass was around 1.0×10^{-4} cm s^{-1} (Figure 7), which was of the same order of magnitude as the transport limited constant for monomer or oligomers ($k_{Lev} \propto D^{2/3} \propto n^{-2/9}$). Although the present analysis was semiquantitative, it was likely that transport played a significant role in the adsorption process of oligomers on hydrophobized glass. In addition, the adsorption kinetics of oligomers on hydrophobized glass did not show a strong pH dependence (Figure 6) in the studied range, whereas the monomer adsorption kinetics were very pH dependent (Figure 4), which emphasized again the qualitative difference of the surface exposed patches of monomer and oligomers.

Conclusion

Scanning confocal fluorescence measurements have been used to investigate the adsorption behavior of the alexa-labeled Bt insecticidal protein, Cry1Aa, on macroscopic flat surfaces of mica and glass. This protein (pI 6.5) has a strong tendency to oligomerize and the adsorption properties of monomer and oligomers have been compared: they were very different.

In contrast with the often reported behavior of globular proteins near their isoelectric point, the adsorption of monomer Cry1Aa toxin was slow on both types of hydrophilic surfaces, mica and glass, and on the hydrophobized glass. It should be pointed out, however, that the nature of the buffer, independent of pH, may play a non-negligible role. The influence of low molecular weight organic acid ligands on toxin adsorption has been studied previously[3] and it was concluded that the binding of the toxin on minerals was looser in the presence of such ions. Inorganic salts can influence also adsorption behavior.[2]

Adsorption of the oligomeric state was greater and decreased in the order hydrophobized glass > mica > hydrophilic glass. The high adsorption of oligomers on the hydrophobic surface may result from neutralizing electric patches in the association that exposes hydrophobic residues in patches facing the hydrophobic surface. On this surface we observed a strong pH dependence for the monomer in contrast to oligomers. The kinetic curve shapes for the monomer on hydrophilic glass differed notably from those of the oligomers. They may be related to conformational changes induced at the interfaces, while similar modifications may already have occurred during the oligomerization process. Whatever the mechanism, the present study suggested that Bt toxin was more easily adsorbed in the oligomer state on various types of surfaces.

This result, obtained with fluorescently tagged protein, suggested faster and greater retention of the toxin in soils if protein aggregation had occurred.

The technique of fluorescence applied here to adsorption studies represents a first step toward determining the profile of concentration in solution near the interface concomitantly to the interfacial concentration as a function of time. Deconvolution of the signal to obtain surface and solution concentrations is presently under investigation. This will lead to a new direct method to determine kinetic parameters that depend on surface availability and adsorption history.[40,41] Still, the present semiquantitative study will become more quantitative with the determination of the ratio V/A and improving the sharpness of transition between the flows of buffer and solution.

Acknowledgment. The authors are grateful for the financial support of Agence Nationale de la Recherche under Contract ANR-05-POGM-002-03. The authors thank R. Frutos for valuable discussion, M. Royer for providing the Bt strain and the cultivation-extraction protocol, F. X. Sauvage for protein analysis, INRA Narbonne for providing the fermentor, and INRA proteomic platform for the mass spectroscopy analyses.

References and Notes

(1) Fu, Q. L.; Deng, Y. L.; Li, H. S.; Liu, J.; Hu, H. Q.; Chen, S. W.; Sa, T. M. *Appl. Surf. Sci.* **2009**, *255*, 4551–4557.
(2) Fu, Q. L.; Wang, W. Q.; Hu, H. Q.; Chen, S. W. *Eur. J. Soil Sci.* **2008**, *59*, 216–221.
(3) Fu, Q. L.; Dong, Y. J.; Hu, H. Q.; Huang, Q. Y. *Appl. Clay Sci.* **2007**, *37*, 201–206.
(4) Helassa, N.; Quiquampoix, H.; Noinville, S.; Szponarski, W.; Staunton, S. *Soil Biol. Biochem.* **2009**, *41*, 498–504.
(5) Zhou, X. Y.; Huang, Q. Y.; Cai, P.; Yu, Z. N. *Pedosphere* **2007**, *17*, 513–521.
(6) Norde, W.; MacRitchie, F.; Nowicka, G.; Lyklema, J. *J. Colloid Interface Sci.* **1986**, *112*, 447–456.
(7) Norde, W.; Anusiem, A. C. I. *Colloids Surf.* **1992**, *66*, 73–80.
(8) Le, M. T.; Dejardin, P. *Langmuir* **1998**, *14*, 3356–3364.
(9) Etheve, J.; Dejardin, P.; Boissiere, M. *Colloids Surf., B* **2003**, *28*, 285–293.
(10) Tapp, H.; Stotzky, G. *Soil Biol. Biochem.* **1998**, *30*, 471–476.
(11) Saxena, D.; Flores, S.; Stotzky, G. *Soil Biol. Biochem.* **2002**, *34*, 133–137.
(12) Tapp, H.; Stotzky, G. *Appl. Environ. Microbiol.* **1995**, *61*, 1786–1790.
(13) Guereca, L.; Bravo, A. *Biochim. Biophys. Acta, Protein Struct. Mol. Enzym.* **1999**, *1429*, 342–350.
(14) Masson, L.; Mazza, A.; Sangadala, S.; Adang, M. J.; Brousseau, R. *Biochim. Biophys. Acta, Protein Struct. Mol. Enzym.* **2002**, *1594*, 266–275.
(15) Walters, F. S.; Kulesza, C. A.; Phillips, A. T.; English, L. H. *Insect Biochem.* **1994**, *24*, 963–968.
(16) Vie, V.; Van Mau, N.; Pomarede, P.; Dance, C.; Schwartz, J. L.; Laprade, R.; Frutos, R.; Rang, C.; Masson, L.; Heitz, F.; Le Grimellec, C. *J. Membr. Biol.* **2001**, *180*, 195–203.
(17) Vasina, E. N.; Dejardin, P. *Biomacromolecules* **2003**, *4*, 304–313.
(18) Vasina, E. N.; Dejardin, P. *Langmuir* **2004**, *20*, 8699–8706.
(19) Vasina, E. N.; Dejardin, P.; Rezaei, H.; Grosclaude, J.; Quiquampoix, H. *Biomacromolecules* **2005**, *6*, 3425–3432.
(20) Borisova, S.; Grochulski, P.; van Faassen, H.; Pusztai-Carey, M.; Masson, L.; Cygler, M. *J. Mol. Biol.* **1994**, *243*, 530–532.
(21) Grochulski, P.; Masson, L.; Borisova, S.; Pusztaicarey, M.; Schwartz, J. L.; Brousseau, R.; Cygler, M. *J. Mol. Biol.* **1995**, *254*, 447–464.
(22) Chevallier, T.; Muchaonyerwa, P.; Chenu, C. *Soil Biol. Biochem.* **2003**, *35*, 1211–1218.
(23) Perrot, H.; Jaffrezic-Renault, N.; Clechet, P. *J. Electrochem. Soc.* **1990**, *137*, 598–602.
(24) Zhuravlev, L. T. *Langmuir* **1987**, *3*, 316–318.
(25) Legrand, A. P. *The Surface Properties of Silicas*; Wiley: Chichester, 1998; p 367.
(26) Balme, S.; Janot, J.-M.; Dejardin, P.; Vasina, E. N.; Seta, P. *J. Membr. Sci.* **2006**, *284*, 198–204.
(27) Lévêque, M. *Les lois de Transmission de la Chaleur par Convection*; Faculté des Sciences: Paris, 1928.
(28) Levich, V. G. *Physical Hydrodynamics*; Prentice-Hall, Inc.: Englewood Cliffs, N.J., 1962.
(29) Dejardin, P.; Le, M. T.; Wittmer, J.; Johner, A. *Langmuir* **1994**, *10*, 3898–3901.
(30) Dejardin, P.; Vasina, E. N. *Colloids Surf., B* **2004**, *33*, 121–127.
(31) Déjardin, P.; Vasina, E. N. Initial adsorption kinetics in a rectangular thin channel and coverage-dependent structural transition observed by streaming potential. In *Proteins at Solid-Liquid Interfaces*; Déjardin, P., Ed.; Springer: Berlin, 2006; pp 51−73.
(32) Yan, F.; Dejardin, P.; Mulvihill, J. N.; Cazenave, J. P.; Crost, T.; Thomas, M.; Pusineri, C. *J. Biomater. Sci., Polym. Ed.* **1992**, *3*, 389–402.
(33) Boumaza, F.; Dejardin, P.; Yan, F.; Bauduin, F.; Holl, Y. *Biophys. Chem.* **1992**, *42*, 87–92.
(34) Robeson, J. L.; Tilton, R. D. *Langmuir* **1996**, *12*, 6104–6113.
(35) Daly, S. M.; Przybycien, T. M.; Tilton, R. D. *Langmuir* **2003**, *19*, 3848–3857.
(36) Daly, S. M.; Przybycien, T. M.; Tilton, R. D. *Colloids Surf., B* **2007**, *57*, 81–88.
(37) Etheve, J.; Dejardin, P. *Langmuir* **2002**, *18*, 1777–1785.
(38) Schaaf, P.; Talbot, J. *J. Chem. Phys.* **1989**, *91*, 4401–4409.
(39) Schaaf, P.; Voegel, J. C.; Senger, B. *J. Phys. Chem. B* **2000**, *104*, 2204–2214.
(40) Calonder, C.; Tie, Y.; Van Tassel, P. R. *Proc. Natl. Acad. Sci. U.S.A.* **2001**, *98*, 10664–10669.
(41) Tie, Y.; Calonder, C.; Van Tassel, P. R. *J. Colloid Interface Sci.* **2003**, *268*, 1–11.

BM100313N